

Potential catalyst savings in heterogeneous gaseous spiral coiled reactor utilizing selective wall coating – A computational study

Jundika C. Kurnia^a, Agus P. Sasmito^{b,*}, Arun S. Mujumdar^{b,c}

^a Department of Mechanical Engineering, Universiti Teknologi PETRONAS, 32610 Bandar Seri Iskandar, Perak Darul Ridzuan, Malaysia

^b Department of Mining and Materials Engineering, McGill University, 3450 University, Montreal, QC, Canada H3A 0E8

^c Department of Chemical and Biochemical Engineering, Western University, Thompson Engineering Building, London, ON, Canada N6A 5B9

ARTICLE INFO

Article history:

Received 21 October 2014

Received in revised form

22 September 2015

Accepted 7 February 2016

Available online 12 February 2016

Keywords:

Catalyst saving

Coiled

Reaction performance

Secondary flow

Selective coating

ABSTRACT

This study numerically evaluates the effect of secondary flow on the reaction performance in heterogeneous gaseous spiral coiled reactor utilizing selective wall coatings. Laminar multispecies gas flow in spiral coiled reactor with circular and square cross-section is investigated using a validated three-dimensional computational fluid dynamics (CFD) model. Various selective wall coating strategies are evaluated within a range of Reynolds number. The reactor performance is measured not only based on the conversion rate but also in terms of figure of merit (FoM) defined as reaction throughput per unit pumping power and catalyst coating active area. The results indicate that secondary flow enhance reaction performance and improve catalyst utilization, especially at the outer wall. By maximizing this effect, the requirement of expensive catalyst materials can be minimized. This study highlight the potential of selective catalyst coating in coiled reactor for process intensification and cost reduction in various applications.

Crown Copyright © 2016 Published by Elsevier Ltd. All rights reserved.

1. Introduction

Due to its compactness, high heat and mass transfer rates and ease of manufacture, coiled/spiral tubes have been widely used in process industries, especially as heat exchangers and chemical reactors. The transport process enhancement in coiled/spiral tube is mainly attributed to the presence of secondary flow as the result of coil/spiral curvature. Aside from engineering application, secondary flow in coiled/spiral duct have attracted considerable attention from engineering researcher due to complex transport phenomena that is associated with it. A large number of experimental and numerical studies have been conducted and reported (Liou, 1992; Kumar et al., 2007; Shokoumand and Salimpour, 2007; Egner and Burmeister, 2005; Kurnia et al., 2012; Naphon and Suwagrai, 2007; Norouzi et al., 2009). In addition, reviews on the flow characteristic and heat transfer performance of coiled tube and its potential applications have been published; for example Naphon and Wongwises (2006), Vashisth and Kumar (2008), and Kumar et al. (2011).

Jayakumar et al. (2010) numerically investigated effect of design parameters, i.e. pitch circle diameter, tube pitch and pipe diameter, with regard to the heat transfer performance. From their study, a correlation to predict Nusselt number based on these design parameters was proposed. Pan et al. (2014) investigated heat transfer characteristic and pressure drop for oscillating flow in helical coil heat exchanger. In their study, the field synergy principle was used to explain the heat transfer enhancement. It was found that better rate of heat transfer can be achieved when the volume average field synergy angle is smaller. In chemical reactor fields, Nigam's group have intensively evaluated coiled tubular reactor and found that the performance of this reactor is in between that of plug and laminar tube flow reactor (Agrawal and Nigam, 2001). Based on their studies, they developed an innovative coiled flow inverter (CFI) design and evaluated its application as an inline mixer (Mandal and Nigam, 2008; Mandal et al., 2011). Realizing the potential of the spiral mini bed reactor developed in their previous study (Kallinikos and Papayannakos, 2007), Kallinikos et al. (2010) utilized the reactor to investigate the kinetic and H₂S effect on the refractory dibenzothiophenes desulfurization in a heavy gasoil. It was found that the spiral reactor was successfully operated even at ultra-deep hydrodesulfurization conditions.

In chemical engineering applications, An et al. (2012) investigated several reactor designs including coiled reactor and found an improved performance in coiled reactor design. Shaker et al.

* Corresponding author. Tel.: +1 514 398 3788; fax: +1 514 398 7099.

E-mail addresses: jundika.kurnia@petronas.com.my (J.C. Kurnia), agus.sasmito@mcgill.ca (A.P. Sasmito).

(2012) evaluated several coiled microreactor designs for mixing and reaction enhancement. They found that secondary flow due to coil curvature improves mass transfer and reaction performance. Solehati et al. (2014) proposed wavy curve micro channel to generate secondary flow to enhance mixing in micro-reactor. Sturm et al. (2013) developed a novel continuous flow coil reactor concept in a rectangular waveguide for the synthesis of n-propyl propionate by esterification of propanol and propionic acid. The results prove that long residence time and high conversion are possible in continuous flow chemistries under single mode microwave field conditions.

In our previous work, mixing, heat transfer and reaction performance of microchannel T-junction with various coiled channels (helical, conical and in-plane) and in-plane spiral microreactor with various cross-section geometry have been investigated (Sasmitho et al., 2012; Kurnia et al., 2014). The results indicated that coiled reactor offers higher reaction performance with the price of higher pressure drop. Among the evaluated cross-sections, circular and square cross-sections provide the highest figure of merit. In that study, all walls of the reactor were coated with catalyst. Meanwhile, it was found that faster reaction rate occurs on the outer wall. Hence it is of interest to selectively coat the wall of spiral reactor and investigate the effect of this treatment to the reaction performance quantitatively. For this purpose, circular and square cross-sections were selected as cases for investigation. The evaluated selective coatings are single wall coating, two wall coating, three wall coating and all wall coating. The objective of this work is to obtain optimum design of spiral reactors while improving catalyst utilization and saving the amount of precious catalyst coating.

2. Mathematical formulation

The studied reactors are spiral coiled reactors with circular and square cross-sections. The schematic representation is presented in Fig. 1 while the details of their geometric parameters are summarized in Table 1. The cross-section areas for all configurations are identical. Several assumptions taken in developing this model are: (i) premix inlet condition; (ii) reaction occurs at the reactor wall; (iii) steady flow; (iv) Newtonian fluid; and (v) laminar flow.

2.1. Governing equations

Based on the assumptions, the conservation equations for mass, momentum and energy for the flow inside the spiral reactor can be expressed as (Sasmitho et al., 2012; Kurnia et al., 2014):

$$\nabla \cdot \rho \mathbf{u} = 0, \quad (1)$$

$$\nabla \cdot (\rho \mathbf{u} \otimes \mathbf{u}) = -\nabla p + \nabla \left[\mu (\nabla \mathbf{u} + (\nabla \mathbf{u})^T) - \frac{2}{3} \mu (\nabla \cdot \mathbf{u}) \mathbf{I} \right], \quad (2)$$

$$\nabla \cdot (\rho \mathbf{u} \omega_i) = \nabla \cdot (\rho D_i \nabla \omega_i) + R_i, \quad (3)$$

$$\nabla \cdot (\rho c_p \mathbf{u} T) = \nabla \cdot (k_{eff} \nabla T) + S_{temp}. \quad (4)$$

Here, ρ is the fluid density, \mathbf{u} is the fluid velocity, p is the pressure, μ is the dynamic viscosity of the fluid, ω_i is the mass fraction of species i , D_i is the diffusion coefficient of species i , R_i is the mass consumed or produced by the reactions at the catalyst coated wall, c_p is the

Table 1
Geometrical parameters.

Parameters	Value	Unit
w	2.00×10^{-2}	m
R_i	2.00×10^{-2}	m
R_o	9.00×10^{-2}	m
d_c	1.13×10^{-2}	m
s	1.00×10^{-2}	m

Table 2
Surface reaction mechanism.

No.	Reaction	A_r	β_r	E_r (J/kmol)
1	$\text{H}_2 + 2\text{Pt}(s) \rightarrow 2\text{H}(s)$	4.36×10^7	0.5	0
2	$2\text{H}(s) \rightarrow \text{H}_2 + 2\text{Pt}(s)$	3.70×10^{20}	0	6.74×10^7
3	$\text{O}_2 + 2\text{Pt}(s) \rightarrow 2\text{O}(s)$	1.80×10^{17}	-0.5	0
4	$\text{O}_2 + 2\text{Pt}(s) \rightarrow 2\text{O}(s)$	2.01×10^{14}	0.5	0
5	$2\text{O}(s) \rightarrow \text{O}_2 + 2\text{Pt}(s)$	3.70×10^{20}	0	2.13×10^8
6	$\text{H}_2\text{O} + \text{Pt}(s) \rightarrow \text{H}_2\text{O}(s)$	2.37×10^8	0.5	0
7	$\text{H}_2\text{O}(s) \rightarrow \text{H}_2\text{O} + \text{Pt}(s)$	1.00×10^{13}	0	4.03×10^7
8	$\text{OH} + \text{Pt}(s) \rightarrow \text{OH}(s)$	3.25×10^8	0.5	0
9	$\text{OH}(s) \rightarrow \text{OH} + \text{Pt}(s)$	1.00×10^{13}	0	1.93×10^8
10	$\text{H}(s) + \text{O}(s) \rightarrow \text{OH}(s) + \text{Pt}(s)$	3.70×10^{20}	0	1.15×10^7
11	$\text{H}(s) + \text{OH}(s) \rightarrow \text{H}_2\text{O}(s) + \text{Pt}(s)$	3.70×10^{20}	0	1.74×10^7
12	$\text{OH}(s) + \text{OH}(s) \rightarrow \text{H}_2\text{O}(s) + \text{O}(s)$	3.70×10^{20}	0	4.82×10^7
13	$\text{CO} + \text{Pt}(s) \rightarrow \text{CO}(s)$	7.85×10^{15}	0.5	0
14	$\text{CO}(s) \rightarrow \text{CO} + \text{Pt}(s)$	1.00×10^{13}	0	1.25×10^8
15	$\text{CO}_2(s) \rightarrow \text{CO}_2 + \text{Pt}(s)$	1.00×10^{13}	0	2.05×10^7
16	$\text{CO}(s) + \text{O}(s) \rightarrow \text{CO}_2(s) + \text{Pt}(s)$	3.70×10^{20}	0	1.05×10^8
17	$\text{CH}_4 + 2\text{Pt}(s) \rightarrow \text{CH}_3(s) + \text{H}(s)$	2.30×10^{16}	0.5	0
18	$\text{CH}_3(s) + \text{Pt}(s) \rightarrow \text{CH}_2(s) + \text{H}(s)$	3.70×10^{20}	0	2×10^7
19	$\text{CH}_2(s) + \text{Pt}(s) \rightarrow \text{CH}(s) + \text{H}(s)$	3.70×10^{20}	0	2×10^7
20	$\text{CH}(s) + \text{Pt}(s) \rightarrow \text{C}(s) + \text{H}(s)$	3.70×10^{20}	0	2×10^7
21	$\text{C}(s) + \text{O}(s) \rightarrow \text{CO}(s) + \text{Pt}(s)$	3.70×10^{20}	0	6.28×10^7
22	$\text{CO}(s) + \text{Pt}(s) \rightarrow \text{C}(s) + \text{O}(s)$	1.00×10^{17}	0	1.84×10^8
23	$\text{OH}(s) + \text{Pt}(s) \rightarrow \text{H}(s) + \text{O}(s)$	1.56×10^{18}	0	1.15×10^7
24	$\text{H}_2\text{O}(s) + \text{Pt}(s) \rightarrow \text{H}(s) + \text{OH}(s)$	1.88×10^{18}	0	1.74×10^7
25	$\text{H}_2\text{O}(s) + \text{O}(s) \rightarrow \text{OH}(s) + \text{OH}(s)$	4.45×10^{20}	0	4.82×10^7

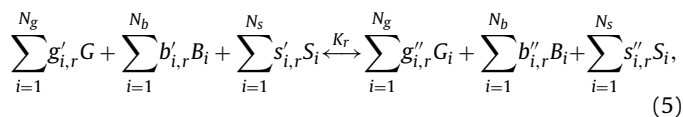
specific heat of the gas mixture, k_{eff} is the effective thermal conductivity, T is the temperature, and S_{temp} is the heat released/absorbed due to reaction.

2.2. Chemical reactions

Similar to our previous work (Sasmitho et al., 2012; Kurnia et al., 2014; Mohan et al., 2014), the reaction considered in this study is heterogeneous reaction of methane oxidation at the microchannel surface coated with a platinum catalyst (Deutschman et al., 2000; Raja et al., 2000; Li, 2009). Other types of reaction processes with established kinetics can also be implemented by using the similar concept.

In this reaction model, chemical species deposited on surfaces is distinguished from the same chemical species in the gas. Similarly, the surface deposition reactions are differentiated from those in the bulk phase even when it involve the same species. The species considered are one bulk/solid species (Pt(b)), seven gas species (CH_4 , O_2 , H_2 , H_2O , CO , CO_2 and N_2), and 11 surface species (e.g. $\text{H}(s)$, $\text{Pt}(s)$, $\text{O}(s)$, $\text{OH}(s)$, $\text{H}_2\text{O}(s)$, $\text{CH}_3(s)$, $\text{CH}_2(s)$, $\text{CH}(s)$, $\text{C}(s)$, $\text{CO}(s)$, $\text{CO}_2(s)$) that illustrate the coverage of the surface with adsorbed species. The detailed multistep reaction mechanism and its reactions rate constants are summarized in Table 2.

Both gas-phase and surface species can be produced and consumed by the surface reaction. The general form of this reaction is written as



where G_i represents the gas-phase species, B_i is the solid species, and S_i is the surface-adsorbed species. Additionally, g' , b' , and s' are the stoichiometric coefficients for each reactant species; g'' , b'' , and s'' are the stoichiometric coefficients for each product species; and K_r is the overall reaction rate constant. Since only the species

Download English Version:

<https://daneshyari.com/en/article/172013>

Download Persian Version:

<https://daneshyari.com/article/172013>

[Daneshyari.com](https://daneshyari.com)